Squaramide-based supramolecular materials Drive hepG2 spheroid differentiation

Liu, T.; Berk, L. van den; Wondergem, J.A.J.; Tong, C.; Kwakernaak, M.C.; Braak, B. ter; ... ; Kieltyka, R.E.

ADVANCED HEALTHCARE MATERIALS
www.advhealthmat.de

Squaramide-Based Supramolecular Materials Drive HepG2 Spheroid Differentiation

*Tingxian Liu, Linda van den Berk, Joeri A. J. Wondergem, Ciqing Tong, Markus C. Kwakernaak, Bas ter Braak, Doris Heinrich, Bob van de Water, and Roxanne E. Kieltyka**

A major challenge in the use of HepG2 cell culture models for drug toxicity screening is their lack of maturity in 2D culture. 3D culture in Matrigel promotes the formation of spheroids that express liver-relevant markers, yet they still lack various primary hepatocyte functions. Therefore, alternative matrices where chemical composition and materials properties are controlled to steer maturation of HepG2 spheroids remain desired. Herein, a modular approach is taken based on a fully synthetic and minimalistic supramolecular matrix based on squaramide synthons outfitted with a cell-adhesive peptide, RGD for 3D HepG2 spheroid culture. Co-assemblies of RGD-functionalized squaramide-based and native monomers resulted in soft and self-recovering supramolecular hydrogels with a tunable RGD concentration. HepG2 spheroids are self-assembled and grown (≈150 µm) within the supramolecular hydrogels with high cell viability and differentiation over 21 days of culture. Importantly, significantly higher mRNA and protein expression levels of phase I and II metabolic enzymes, drug transporters, and liver markers are found for the squaramide hydrogels in comparison to Matrigel. Overall, the fully synthetic squaramide hydrogels are proven to be synthetically accessible and effective for HepG2 differentiation showcasing the potential of this supramolecular matrix to rival and replace naturally-derived materials classically used in high-throughput toxicity screening.

The liver is a critical organ of the human body that performs the biotransformation of drugs and other xenobiotics. Chemical transformations, such as oxidation, reduction, hydrolysis or other organic reactions, of these foreign agents give rise to active or inactive metabolites that can even be hepatotoxic.[1] Toxic insults to the liver from drug metabolites can eventually result in acute or chronic failure, otherwise known as drug-induced liver injury (DILI). DILI can occur from nearly every class of medication, and when encountered often results in abandonment of the therapy.[2] Thus, a major challenge in the drug discovery pipeline is to more accurately predict DILI early on, as hepatotoxic responses observed in animal models do not fully recapitulate those observed in humans resulting in drug candidates that fail in late stage clinical trials or even after approval in the clinic.[3]

Primary human hepatocytes (PHH) are the current gold standard for in vitro modeling of liver metabolism and toxicity as they represent 70% of total liver cell population. However, these cells are challenged by their limited availability and high donor variability, rapid loss of metabolic activity once harvested for ex vivo culture and costly derivation.[4,5] As an alternative cell source to model liver hepatic processes in vitro, human liver carcinoma cells (HepG2) are used due their wide availability, immortality, facile handling, and stable phenotype in culture. However, these cells often show low expression levels of metabolic enzymes, namely cytochrome P450s that are relevant for xenobiotic metabolism, which has

T. Liu, Dr. C. Tong, M. C. Kwakernaak, Dr. R. E. Kieltyka
Department of Supramolecular and Biomaterials Chemistry
Leiden Institute of Chemistry
Leiden University
P.O. Box 9502, Leiden 2300 RA, Netherlands
E-mail: r.e.kieltyka@chem.leidenuniv.nl

L. van den Berk, Dr. B. ter Braak, Prof. B. van de Water
Division of Drug Discovery and Safety
Leiden Academic Centre for Drug Research
Leiden University
P.O. Box 9502, Leiden 2300 RA, Netherlands

J. A. J. Wondergem, Prof. D. Heinrich
Department of Physics
Huygens-Kamerlingh Onnes Laboratory
Leiden University
Leiden 2300 RA, Netherlands

J. A. J. Wondergem, Prof. D. Heinrich
Fraunhofer Institute for Silicate Research ISC
Neunerplatz 2, Würzburg 97082, Germany

The ORCID identification number(s) for the author(s) of this article can be found under https://doi.org/10.1002/adhm.202001903

DOI: 10.1002/adhm.202001903

been correlated with the 2D culture methods used to expand them.[6] 3D culture methods have been used to improve the metabolic characteristics of HepG2 cells mainly using Matrigel, a biological matrix derived from murine tumor tissues, consisting of laminin, collagen IV, and entactin.[7] When encapsulated in Matrigel, HepG2 cells self-organize into spheroidal structures and differentiate resulting in increased levels of various metabolic markers and can be dosed repeatedly with increased sensitivity to various hepatotoxic agents in comparison to HepG2 cells cultured in 2D.[8,9] However, Matrigel is costly, lacks definition with lot-to-lot variability,[7] its murine origin is problematic for some applications and chemical modification or decoupling of cues is difficult, leading to the exploration of synthetic polymers for use in 3D hepatocyte culture.

Matrices held together by covalent and non-covalent interactions have demonstrated the capacity to form spheroids from liver-derived cells in 3D, including a handful of recent reports examining the effect of cell interactive moieties to facilitate their differentiation and culture with varying degrees of success.[10–19] More recent studies have examined the capacity of the short integrin-binding peptide RGD to guide this process highlighting the importance of peptides derived from extracellular matrix proteins in synthetic materials. While a fully synthetic and covalent PEG hydrogel functionalized with RGD supported the growth of liver organoids, the addition of laminin–entactin complex was necessary for a non-covalent hydrogel based on a polyisocyanopeptide polymer to stimulate cell proliferative pathways demonstrating the importance of peptide concentration.[17,18] We thus became interested in examining a modular supramolecular polymer matrix based on stacked monomers for HepG2 cell culture to improve their growth and differentiation in 3D. However, such supramolecular systems that have the short peptides derived from matrix proteins is yet to be explored for the preparation of HepG2 spheroids, but can more broadly provide a powerful synthetic polymer platform for 3D cell culture where the peptide concentration can be tuned easily and facile cell seeding and release can be achieved.

In order to construct supramolecular polymer materials, monomers that contain highly directional, specific, and reversible non-covalent interactions are needed.[20–24] In particular, squaramide synthons because of their ditopic presentation of hydrogen bond donors and acceptors on a minimal scaffold in combination with their synthetic accessibility are of interest for this aim.[25–32] We recently demonstrated their application in a tripodal hydrogelator for the culture of human induced pluripotent stem cells (hiPSCs), using the soft and self-recovering nature of the supramolecular matrix that supports cell self-assembly into spheroids driven by cell–cell contacts.[31] However, cell proliferation within these materials was found to be limited, pointing out the need to further modify this synthetic matrix with bioactive peptides to enable cell–matrix interaction. One short peptide that has been implemented in materials to provide such interactions is the RGD peptide, a short sequence derived from the FN-III repeat in the tenth domain of fibronectin, that binds the $\alpha 5\beta 1$ and $\alpha V\beta 3$ integrins on the cell surface. We therefore sought to introduce this cell-adhesive peptide within squaramide-based supramolecular materials through co-assembly of functional monomers as a facile means to tune peptide concentration for applications in 3D HepG2 culture and differentiation.

Earlier, we designed a tripodal squaramide-based monomer (**1**) where three squaramides were embedded within a hydrophobic core consisting of tris(2-aminoethylamine) (TREN), aliphatic, and a peripheral hydrophilic domain with oligo(ethylene glycol) chains. In this study, we further sought to incorporate the RGD peptide into these squaramide monomers (**2**) to aid in cell proliferation, but also to provide a cell adhesive contact for cells. (**Scheme 1**) However, the lack of reactive handle, namely the terminal methyl group on the oligo(ethylene glycol) chains of the monomer preclude it from further functionalization with any cargo, such as fluorescent dyes, crosslinkers, peptides, or proteins. Therefore, a desymmetrized tripodal squaramide-based monomer where one of the three arms was end-functionalized with an azide (**3**) was designed and synthesized starting from a monotrityl-protected TREN core. The azide functionality was first introduced onto tetraethylene glycol by tosylation. (Scheme S1, Supporting Information)[33] The tetraethylene glycol monomethyl ether and monoazide tetraethylene glycol were then independently activated using 1,1-carbonyldiimidazole and further reacted with monotrityl-protected C10 diamine in presence of *N*,*N*-Diisopropylethylamine (DIPEA) resulting in yields of 63% (methyl-terminated) and 74% (azide-terminated), respectively. The trityl protecting group was deprotected by TFA under an inert atmosphere, followed by its subsequent reaction with dibutyl squarate to provide the methyl-terminated and azide-terminated squaramide amphiphiles in yields of 87% and 47%, respectively. (Scheme S2, Supporting Information) Subsequently, the methyl-terminated squaramide amphiphile was reacted onto the desymmetrized TREN core resulting in a yield of 54%. Last, the trityl group on TREN core was deprotected using TFA and further coupled to the azide-terminated squaramide amphiphile giving the final compound **3** in a 56% yield. (Scheme S3, Supporting Information) The RGD peptides (GGGRGDS, PEP1) were then synthesized by solid-phase peptide synthesis with the introduction of 4-pentyonic acid at the N-terminus to provide a reactive handle for bioconjugation. In a final step, the alkyne-ended RGD peptides (PEP2) were coupled to **3** by copper(I)-catalyzed azide–alkyne cycloaddition (CuAAc) obtaining the peptide-functionalized squaramide monomer **2** (Scheme S4, Supporting Information). Monomers **1** and **2** were purified by high performance liquid chromatography (HPLC) prior to self-assembly and gel preparation. Detailed synthetic information can be found in the Supporting Information.

For subsequent 3D cell culture studies, a supramolecular co-assembly protocol was developed to mix both native monomer **1** and RGD-functionalized squaramide monomer **2** (Scheme 1A and Figure S1, Supporting Information). DMSO stock solutions of monomers **1** and **2** were first prepared at concentrations of 25 and 5 mM, respectively, followed by mixing in a controlled and tunable manner based on concentration and volume calculations. The DMSO mixture was then exposed to nitrogen flow overnight to obtain a dried film. Afterward, hydrogel preparation was performed by rehydration in PBS, vortexing, and sonication in an ice–water bath (4 °C, ≈30 min). Last, the obtained transparent solution was incubated at 37 °C for 30 min and equilibrated overnight prior to further use for subsequent experiments.

UV–vis spectroscopy measurements were performed to understand the effect of the mixing protocol on the functional squaramide-based supramolecular monomers and mixtures at

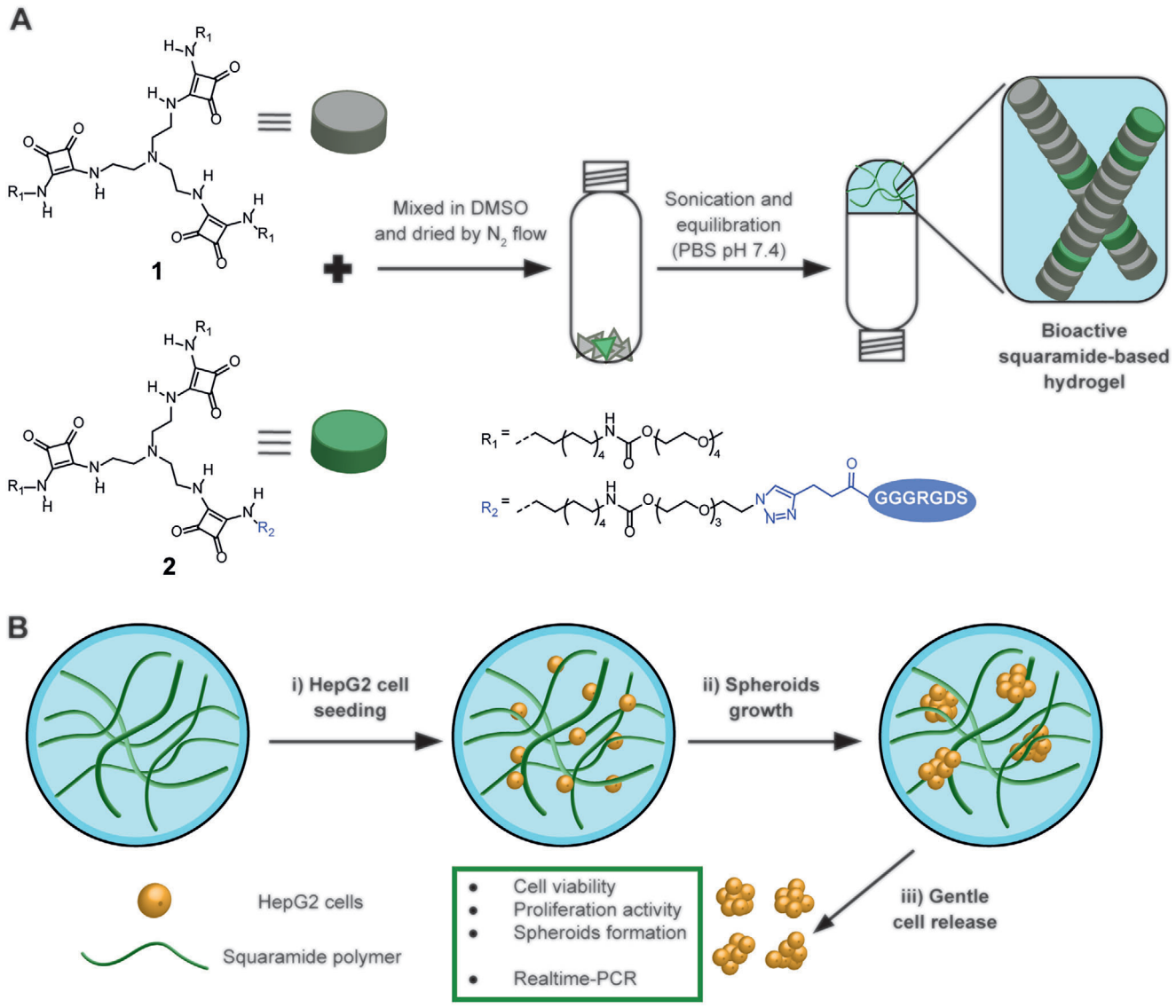

Scheme 1. A) Preparation of bioactive squaramide-based supramolecular hydrogels: native tripodal squaramide monomer (**1**) was mixed with an RGD-functionalized monomer (**2**) in DMSO. The dried solid was rehydrated in phosphate buffered saline (PBS, pH 7.4) by sonication, followed by being left to equilibrate overnight to obtain the co-assembled bioactive hydrogels. B) HepG2 spheroids cultured in bioactive squaramide-based supramolecular hydrogel for 21 days: i) HepG2 cells were mixed and encapsulated within the hydrogel by pipetting using its self-recovery property; ii) HepG2 cells self-assemble into spheroids, proliferate, and differentiate within the hydrogel; iii) HepG2 spheroids were released by dilution and used for further analysis including cell proliferation and gene expression.

the molecular level. UV–vis spectra of both monomer **1** and **2** in DMSO showed a single band at 293 nm that consistent with depolymerization of the squaramide monomers (Figure S1, Supporting Information).[29] After rehydration of the films in PBS, samples containing 2, 5, 10, and 15 mol% of monomer **2** (SQ-2RGD, SQ-5RGD, SQ-10RGD, and SQ-15RGD) displayed two absorption bands at 262 and 322 nm corresponding to the HOMO−LUMO+1 and HOMO−LUMO transitions of squaramide, respectively. (Figure S5, Supporting Information)[29,31] These bands are identical to the supramolecularly polymerized monomer **1** on its own suggesting that the mixing of monomer **2** up to 15 mol% does not modify its aggregation at the molecular level. However, further increasing the amount of monomer **2** up to 40 mol%, the HOMO−LUMO+1 and HOMO−LUMO transitions were recorded at 267 and 319 nm, pointing to a slightly lower degree of aggregation compared to the native monomer **1**. Together these results suggest DMSO depolymerizes the squaramide monomers, including those with the RGD peptide functionality, and repolymerization is achieved when prepared as co-assemblies in buffered solutions.

RGD-functionalized squaramide hydrogels were prepared with various mol% of monomer **2** and their capacity to gelate water was first approximated by a gel inversion test. The total squaramide monomer concentration was maintained at 3.1 mM and the effect of increasing the amount of monomer **2** on co-assembly was examined (0.06–0.45 mM RGD peptides).

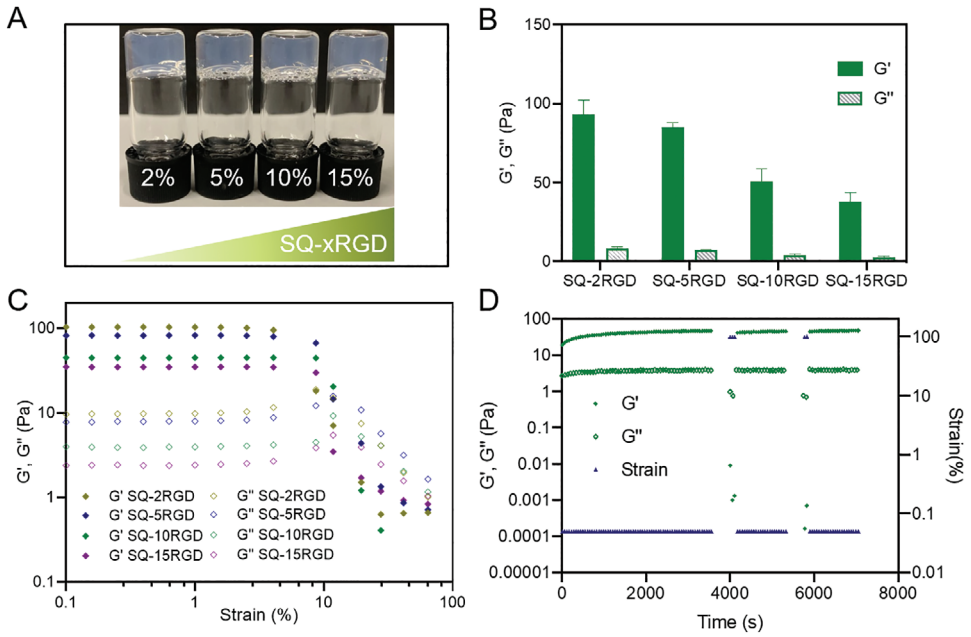

Figure 1. A) Gel inversion test of RGD-functionalized squaramide hydrogels (3.1 mM) prepared in PBS (pH 7.4) SQ-xRGD: hydrogels containing *x* mol% of the monomer **2**. Oscillatory rheology measurements: B) Averaged ($N = 3$) storage (G') and loss (G'') moduli of hydrogels (3.1 mM, PBS) collected at 37 ± 0.2 °C by a time-sweep measurement with a fixed frequency of 1 Hz and strain of 0.05%. C) Amplitude sweep of RGD-functionalized squaramide hydrogels at 37 ± 0.2 °C with a frequency of 1 Hz and strain from 0.1% to 100%. D) Step-strain measurements of hydrogel SQ-10RGD (3.1 mM) at 37 ± 0.2 °C with a frequency of 1 Hz. Frequency-sweep measurements (from 0.01 to 2 Hz, $\gamma = 0.05\%$) were performed between application of low (0.05%) and high strain (100%) (data not shown).

(**Figure 1**A) Non-flowing hydrogel materials were observed up to 15 mol% **2**. The mechanical properties of RGD-functionalized squaramide hydrogels were further assessed quantitatively by performing oscillatory rheology. From the time sweep measurements, hydrogel formation was confirmed with storage moduli (G') being greater loss moduli (G'') for the various samples. Mechanically soft hydrogels were formed for all compositions with a G' lower than 100 Pa; a decreasing trend was observed with the increase of monomer **2**. (Figure 1B) An amplitude sweep experiment in a range of strain from 0.1% to 100% was used to determine the linear viscoelastic (LVE) region of the various materials. In the case of hydrogels SQ-2RGD and SQ-5RGD, G' and G'' remained constant until 4% strain, whereas for hydrogels SQ-10RGD and SQ-15RGD the exit from the linear regime was observed at 6% strain. (Figure 1C) Moreover, frequency sweep measurements showed rheological profiles consistent with viscoelastic materials in a frequency range from 0.01 to 2 Hz for all hydrogels up to 15 mol% monomer **2** with G' was greater than G'' by an order of magnitude (Figure S2, Supporting Information). Last, step-strain measurements were executed to evaluate the effect of the added monomer **2** on the self-recovery properties of the supramolecular hydrogels. With the addition of monomer **2** up to 15 mol%, the RGD-functionalized squaramide hydrogels showed similar self-recovery behavior to the previously reported native hydrogel SQ, namely the decrease and inversion of both moduli (G' and G'') in response to large amplitude strain, and recovery of the material to its initial state after its removal over two cycles.[31] (Figure 1D and Figure S3, Supporting Information) To better understand the effect of increasing peptide monomer concentration, a sample with a greater mol percentage of monomer **2** (SQ-40RGD) was examined. While $G' > G''$ in time sweep measurements, G' and G'' were found to decrease ($G' = 1.26$ Pa, $G'' = 0.27$ Pa) significantly (Figure S4, Supporting Information) demonstrating a negative effect of the peptide monomer on gelation properties.

Further insight into the origin of the measured rheological properties was provided by cryogenic transmission electron microscopy (cryo-TEM). As shown in Figure S5, Supporting Information, flexible, micron-length nanofibers were observed for SQ-10RGD hydrogels (3.1 mM, PBS) indistinguishable from the SQ hydrogels with a slightly smaller width of 4.8 ± 0.4 nm. Because of the difference in gel rheological properties with increasing peptide concentration, we further examined the effect of increasing monomers **2** on the nanoscale structure of the squaramide-based supramolecular polymer fibers. Similarly, entangled fibers were observed in SQ-40RGD solution, with comparable fiber width of 4.6 ± 0.6 nm, indicating that the co-assembly of monomer **2** was comparable at the nanoscale level. (Figure S6, Supporting Information)

RGD peptides bind cell-surface integrins and through these receptors they stimulate actin polymerization upon cell attachment, facilitating cell spreading and contractile movements.[34,35] Therefore, before applying the co-assembled supramolecular polymers for 3D cell culture, we first investigated whether cells can recognize and respond to the RGD peptides presented by the squaramide-based polymers. Consequently, NIH3T3-LifeAct-mCherry cells transduced to express m-Cherry-labeled actin were encapsulated and cultured in squaramide-based hydrogels. Branched, large protrusions (pseudopods) tipped with actin rich filopodia outside of the cell body were observed

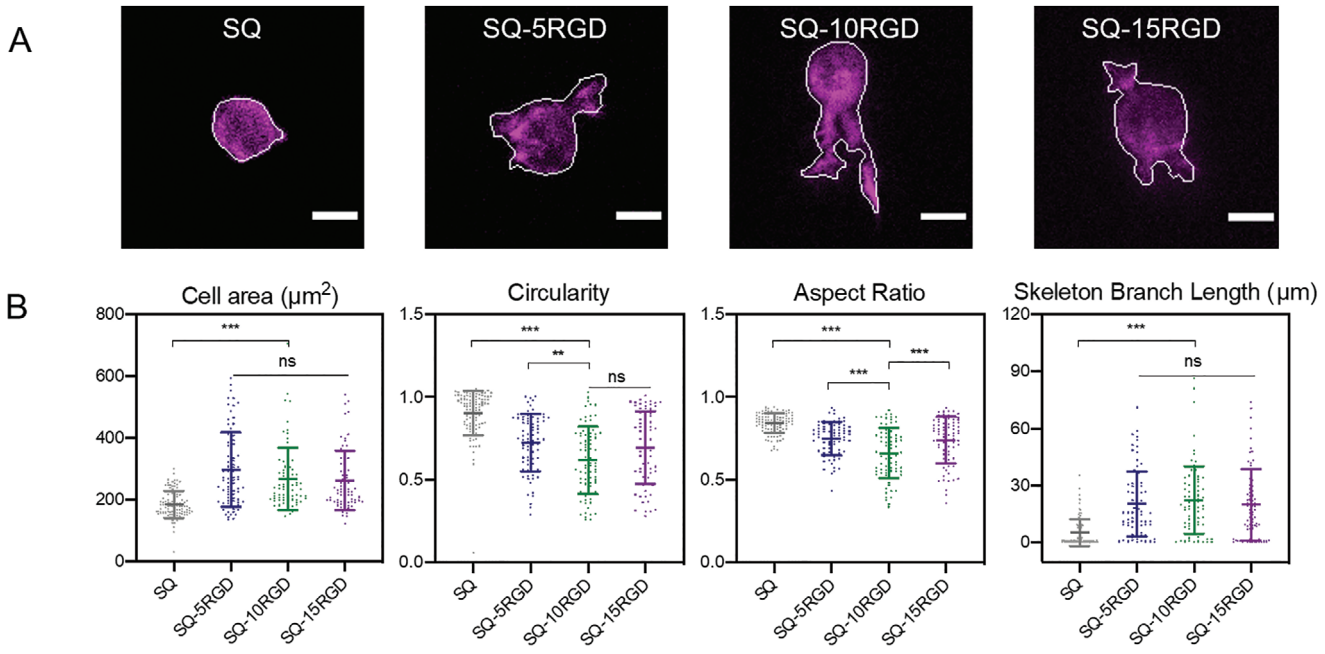

Figure 2. A) Representative images of NIH3T3-LifeAct-mCherry cells cultured within squaramide-based hydrogels after 24 h, scale bar: 10 μm; B) Quantitative analysis of mean projected cell area, perimeter, circularity, and skeleton branch length from NIH3T3-mCherry-LifeAct cells cultured for 24 h within squaramide-based hydrogel. For each data set, 74–100 cells were analyzed. The mean and standard deviation are marked within the graphs. (*$P < 0.05$, **$P < 0.01$, ***$P < 0.001$ one-way Anova)

in the SQ-10RGD and SQ-15RGD hydrogels, as previously reported in ECM-derived collagen hydrogels.[36,37] (Videos S1 and S2, Supporting Information) Additional to protrusion formation, cell migration was also observed indicating extensive cell-hydrogel interactions in 3D. In contrast, cells in native SQ hydrogels displayed a highly rounded morphology, with minimal spreading and were rarely observed to migrate. (Video S3, Supporting Information) This indicates that the inclusion of RGD peptides is essential for cell spreading and migration in the squaramide-based supramolecular hydrogel. To further quantify cell spreading efficiency as a function of RGD concentration, cells were cultured in squaramide-based hydrogels for 24 h and then subsequently imaged (2.5 μm stepped *z*-stacks). Using image analysis, all cells in each imaged volume slice were recognized and a local 2D *z*-projection was made around each cell to individually analyze and extract appropriate cell edges. The cell edges were used to calculate morphological parameters such as cell area, perimeter, circularity, summated skeleton branch length, min- and max Feret diameter, and aspect ratio. Cells tended to spread significantly more in RGD-functionalized squaramide hydrogels, as shown in **Figure 2**A and Figure S8, Supporting Information, and quantitatively displayed larger cell areas and longer perimeters in comparison to those in SQ ($P < 0.001$, Figure 2B and Figure S8, Supporting Information). Consistently, cell circularity was much lower in RGD-functionalized hydrogels, calculated to be 0.726, 0.619, and 0.694 for cells in SQ-5RGD, SQ-10RGD, and SQ-15RGD, respectively, in comparison to that in SQ (0.903). To gather further information of cell protrusion formation, the cell shapes were skeletonized, the Feret diameters were measured and aspect ratios were calculated. Significantly larger Feret diameters were observed for cells cultured in RGD-functionalized hydrogel in comparison to that in SQ ($P < 0.001$), supporting cell elongation within the RGD-presenting materials. Among them, the lowest aspect ratio was calculated from cells cultured in SQ-10RGD, as shown in Figure 2B. Moreover, the summated skeleton branch lengths for each cell, used as an indicator of protrusion length, was found to be 22.4 ± 3.3 μm in SQ-10RGD, a 4-fold increase over that in SQ (5.2 ± 1.2 μm). (Figure 2B and Table S1, Supporting Information) Taken together, the cells displayed a more spread and branched morphology with highly dynamic actin polymerization along the cell membrane, especially at the end of branched protrusions as a consequence of interaction with RGD peptides in the bioactive squaramide-based hydrogels as previously reported in literature powering cell migration within the hydrogels.[34]

The aggregation of HepG2 cells into spheroidal structures that resemble their presentation in vivo provide a versatile tool to investigate hepatic metabolism, stemness, cancer, and chemical safety assessment.[38–40] Because bioactive squaramide-based hydrogels containing an RGD-ligand support active cell migration and proliferation, we became interested if these materials would further enable the self-assembly of HepG2 cells into spheroids and facilitate their differentiation. A recent study demonstrated that low concentrations of RGD peptide (≈0.2 mM) may be not sufficient for human liver organoid proliferation,[17] thus bioactive squaramide-based hydrogels were examined at 0.3 and 0.45 mM RGD with hydrogels lacking the RGD monomer **2** and Matrigel being used as controls. As expected, HepG2 cells grew within SQ-10RGD hydrogel by starting from single cells (1×10^5 cells mL^{-1}) on day 3 to small aggregates on day 7, and finally, rounded spheroids on day 14 that continued to increase slightly in size until day 21. (**Figure 3**A) HepG2 cells grew similarly in

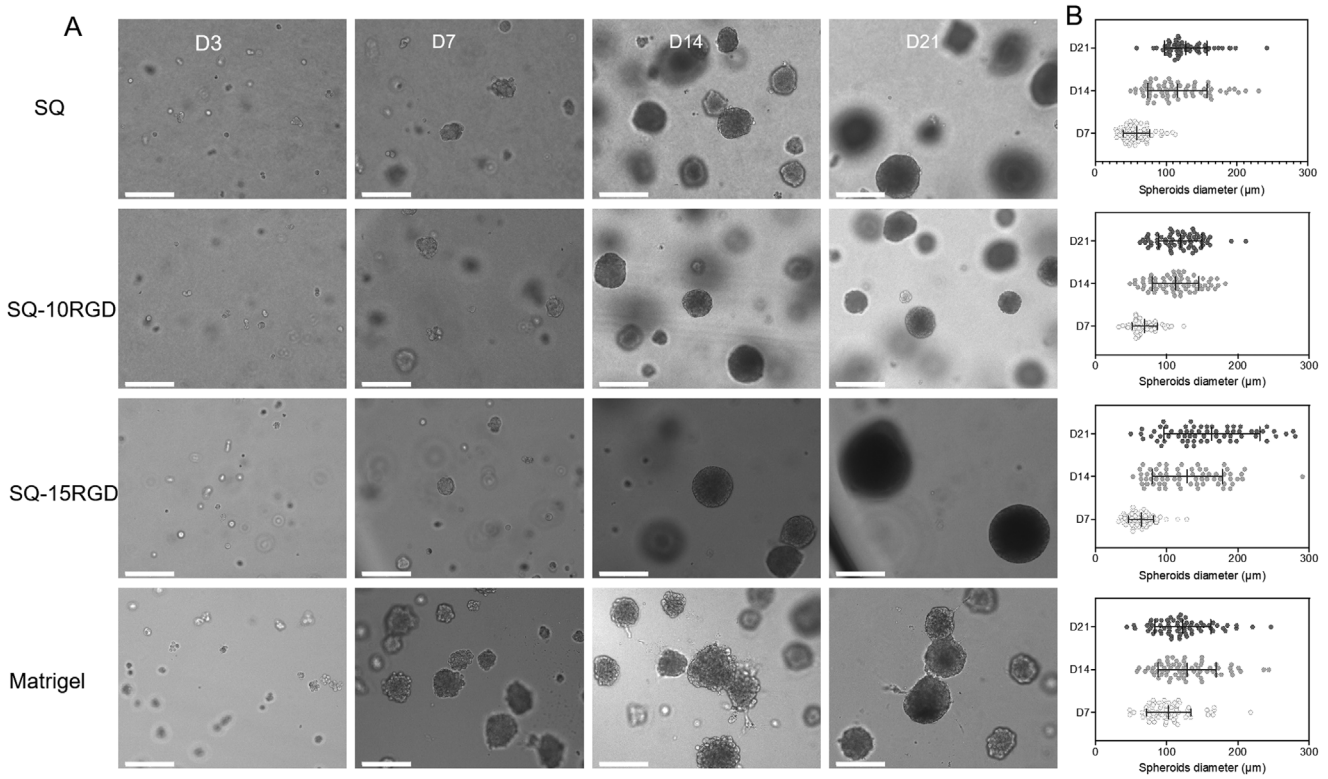

Figure 3. 3D HepG2 cell culture in squaramide-based hydrogels over a 21-day period. A) Bright field images taken on day 3 (D3), 7 (D7), 14 (D14), and 21 (D21). Scale bar: 200 μm. B) Size distribution of HepG2 spheroids during the 21-day culture period in squaramide-based hydrogels and Matrigel (LOT5215008). For each group, 66 spheroids were measured in Fiji by manually drawing a straight line horizontally (angle < 3°). The means and standard deviations are marked inside the graphs.

SQ and SQ-15RGD hydrogels forming compact spheroids on day 14. As a control, spheroids cultured in Matrigel, the current gold standard cell culture matrix, displayed a slightly less compacted morphology throughout the culture period. Spheroid diameter was measured to quantitatively compare the performance of the supramolecular matrix against Matrigel in generating these morphological structures. Increase in the spheroidal diameter over the 21-day culture period was confirmed by plotting the measured size distributions in Figure 3B. Cellular aggregates of 58 ± 18, 69 ± 17, and 64 ± 17 μm were obtained on day 7 in SQ, SQ-10RGD and SQ-15RGD hydrogels, and grew into spheroids with diameters of 116 ± 40 μm, 112 ± 32 μm, and 129 ± 49 μm on day 14, respectively. From day 14 to day 21, spheroids in SQ and SQ-10RGD hydrogels were comparable in diameter, 127 ± 30 μm and 119 ± 30 μm, respectively. Conversely, HepG2 cells cultured in Matrigel formed spheroids with average diameter of 102 ± 31 μm on day 7 and increased in size to 128 ± 40 μm on day 14 and 122 ± 22 μm on day 21, respectively. From all hydrogel conditions tested, the HepG2 spheroids in SQ-15RGD hydrogel displayed highest diameters at 163 ± 66 μm on day 21, yet remained below 200 μm providing sufficient oxygen diffusion throughout the spheroid.[41,42] This increase in spheroid diameter in the squaramide-based hydrogels suggests proliferation of HepG2 cells during the culture period.

Proliferation of the HepG2 spheroids cultured in the bioactive squaramide-based hydrogels were further assessed by their imaging with 5-ethynyl-2′-deoxyuridine (EdU). In order to facilitate their staining, the HepG2 spheroids were released from the hydrogels by dilution of the supramolecular matrix at predetermined time points, imaged and analyzed quantitatively for EdU positive cells. Proliferative cells were observed to be randomly distributed throughout the HepG2 spheroids suggesting that sufficient nutrient diffusion through squaramide-based hydrogels and the spheroids occurs during culture. (**Figure 4**B) In the SQ hydrogel lacking RGD peptides, HepG2 cells displayed comparable proliferative activity based on the EdU-positive percentage over the culture period, namely 18 ± 16.2% on day 7, 8 ± 6.4% on day 14, and 10 ± 6.2% on day 21, respectively. In the RGD-functionalized squaramide-based hydrogel, HepG2 cells were found to proliferate actively at the beginning of the culture period with the measured percentage of EdU-positive cells on day 7 being 25 ± 9.9% and 45 ± 8.4% in SQ-10RGD and SQ-15RGD hydrogels, respectively. Notably, HepG2 cells cultured in Matrigel displayed an EdU-positive percentage of 41 ± 12.8% on day 7 that declined to 7 ± 5.0% on day 14 and eventually ended at 6 ± 5.2%. As the culture progressed from day 7 to 14 in both Matrigel and squaramide hydrogels, a dramatic decrease in the percentage of EdU-positive cells was measured pointing to decreased proliferation and suggestive of their differentiation. SQ-15RGD showed the highest proliferation of the HepG2 cells in comparison to Matrigel, SQ and SQ-10RGD hydrogels on day 14, and is consistent with the significantly larger measured diameter of the spheroids. In the case of SQ-10RGD and SQ-15RGD slightly increased proliferation of 13 ± 9.2% and 14 ± 2.8%, respectively,

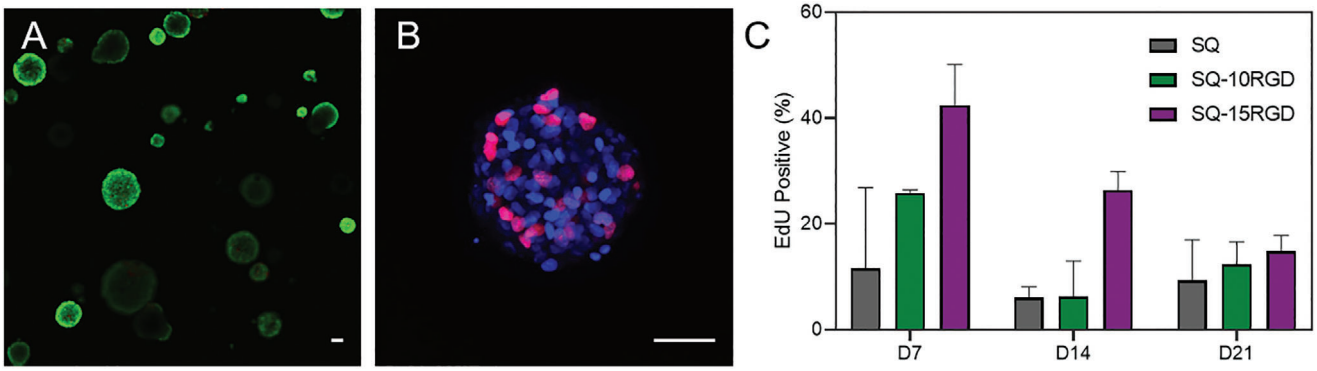

Figure 4. A) Cell viability assay of HepG2 spheroids cultured in SQ-10RGD hydrogel for 21 days stained by a LIVE/DEAD assay with calcein AM (viable cells, green) and propidium iodide (PI) (dead cells, red). B) EdU staining of released HepG2 spheroids cultured in SQ-10RGD hydrogels. Proliferating cells were labeled with EdU-Alexa fluor 594 (red) and cell nuclei were stained with Hoechst 33 342 (blue). Scale bar: 50 μm. C) Quantification of EdU percentage in HepG2 spheroids cultured within Matrigel, SQ, SQ-10RGD, and SQ-15RGD hydrogels. $N = 3$.

was recorded at the end of culture and is slightly greater than for the SQ monomer (10 ± 6.2%). (Figure 4C and Figure S10, Supporting Information) Besides the early active cell proliferation, HepG2 spheroids cultured within squaramide-based hydrogels were largely calcein AM positive with few dead cells confirming high cell viability and the absence of a necrotic core during the culture. (Figure 4A and Figure S9, Supporting Information) Collectively, RGD-functionalized squaramide hydrogels support the formation of HepG2 spheroids with a size greater than 150 μm initially showing active cell proliferation that decreases toward the end of the 21-day culture period. The initial increased cell proliferation could further affect HepG2 cell differentiation resulting in the induction of metabolic enzymes and expression of hepatic markers.

HepG2 cells showed spheroid formation in SQ, SQ-10RGD, and SQ-15RGD hydrogels with high cell viability and increased proliferation in the bioactive gels early on in the culture. However, it was previously demonstrated that the formation of these in vivo mimicking structures in 3D in peptide nanofiber hydrogel-based does not necessarily result in the distinct expression of metabolizing enzymes by RT-PCR.[11] Consequently, to assess the bioactive squaramide-based materials on the maturation of HepG2 spheroids, RT-PCR experiments were performed to evaluate the expression of a panel of metabolic enzymes and hepatic markers. As hypothesized, the HepG2 spheroids showed higher expression of various phase I and II metabolic enzymes and drug transporters in the 3D cultures performed in comparison to 2D. (**Figure 5**A) mRNA expression of CYP1A2 measured from cells cultured in 3D in the Matrigel matrix control was over 40-fold in comparison to the 2D condition. Similarly, both CYP2C19 and CYP3A4 showed an over tenfold enhancement in 3D in comparison to 2D culture and CYP2C9 and CYP2D6 expression was increased 3- and 4.5-fold, respectively. Additionally, mRNA levels of the phase II xenobiotic-metabolizing enzymes UGT1A1 increased by over 45-fold and expression of hepatic markers HNF4a and NCTP were also found to increase over two times during hydrogel-based culture. The overall higher gene expression of metabolic enzymes and hepatic markers are consistent with previous reports that the formation of compact spheroids in 3D are beneficial for hepatocyte maturation.[8,12] When compared against the HepG2 spheroids cultured in Matrigel, cells cultured in the bioactive squaramide-based hydrogel SQ-10RGD in 3D displayed significantly higher mRNA expression in case of CYP2D6 (4.7-fold), CYP2C19 (4.2-fold), CYP2C9 (3.6-fold), and NCTP (4.9-fold) and comparable level in CYP1A2 (1.8-fold), UGT1A1 (1.4-fold), CYP3A5 (1.5-fold), and HNF4a (1.5-fold). These results strongly suggest that the fully synthetic bioactive squaramide-based hydrogel can function well as an alternative matrix of Matrigel for HepG2 culture. More importantly, in comparison to the control SQ hydrogel, cells were cultured within SQ-10RGD hydrogel displayed significant improved mRNA expression of NCTP ($^{**}P < 0.01$) and advantageous expression of CYP2D6, CYP2C19, CYP1A2, HNF4a, and UGT1A1, confirming the importance of incorporating bioactive peptides to further stimulate differentiation. The overall enhancement in gene expression in HepG2 spheroids by introducing RGD peptides is less obvious than that of transferring cells from 2D to 3D culture, implying cell–cell contact plays a critical role in their differentiation rather than cell–matrix interactions, at least under the tested cell seeding condition.[43,44] However, matrix proteins have been earlier demonstrated to play an important role in the assembly of HepG2 spheroids and this can also explain the subtle increases between the RGD and native conditions.[45]

To further probe the differentiation of spheroids in 3D in squaramide-based hydrogels, immunostaining of albumin, and bile canaliculi-like structures through MRP2 was performed (Figure 5B and Figure S12, Supporting Information).[8,9] Albumin expression was present in both Matrigel and squaramide-based hydrogels culture systems. In contrast, MRP2 expression was localized in actin-rich regions suggesting bileduct formation, with a more intense staining in hepG2 spheroids that were cultured in SQ and SQ-10RGD hydrogels in comparison to those in Matrigel. Conversely, MRP2 staining was hardly observed in spheroids from the SQ-15RGD hydrogel that had the largest aggregates. Moreover, β-catenin expression at the borders of the hepG2 spheroids indicate that independent of the gel used the cells establish basal-lateral polarity.

To summarize, the quantified mRNA expression of metabolic enzymes and hepatic makers from HepG2 cells cultured in squaramide-based hydrogels confirms our hypothesis that our bioactive and chemical-defined synthetic matrix can be an alternative to Matrigel to support their 3D cell culture, and

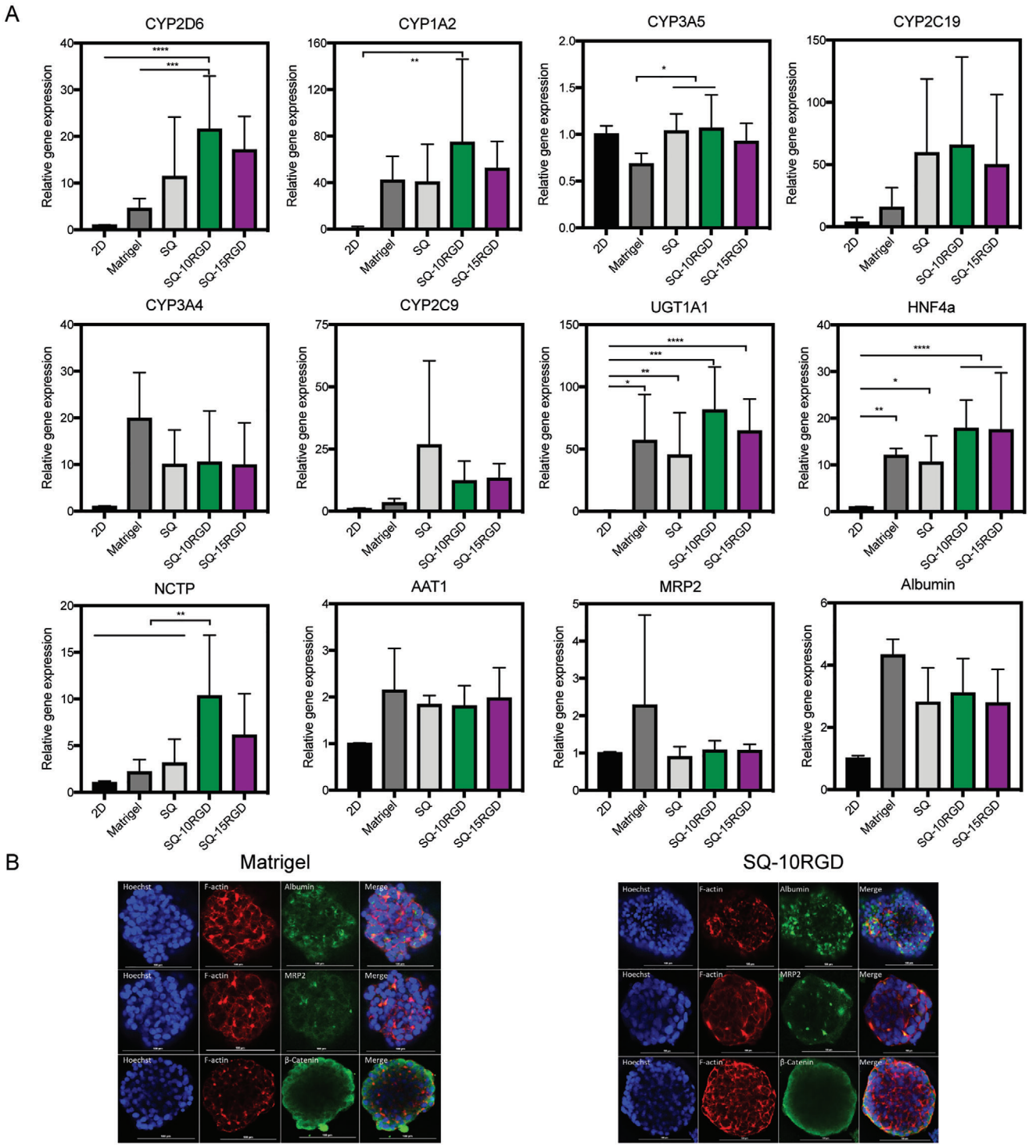

Figure 5. A) Real-time PCR analysis of metabolic enzymes and liver-specific markers in 2D and 3D culture. Fold change gene expression levels of HepG2 spheroids after 3D culture for 21 days compared to 2D culture for 3 days. Data are collected from three biological replicates. (*$P < 0.05$, **$P < 0.01$, ***$P < 0.001$, ****$P < 0.0001$ one-way Anova). B) Immunofluorescence staining of the liver markers albumin (upper row), MRP2 (middle row) and β-catenin (lower row) in green, and counter-stained with F-actin rhodamine phalloidin (red) and the nuclear stain Hoechst33342 (blue). Merged channels consist of all three stainings. Scale bar: 100 µm.

importantly, incorporation of cell adhesion motifs (RGD) enhanced cell proliferation, and thus improve cell hepatic makers expression in 3D. Still, as observed from real-time PCR analysis in Figure 5A, some variation between biological replicates was observed in the gene expression, which was comparable to that of Matrigel from different lots (Figure S11, Supporting Information), especially with respect to CYP1A2 and UGT1A1 expression. Likely these variations are due to the non-uniform size of the formed spheroids in 3D within the materials that influence the metabolic activity of the HepG2 cells and further refinement of the overall synthetic matrix composition and/or culture protocol will require methods to control spheroid size prior to cell culture within the materials.[46,47] Gratifyingly, this fully synthetic supramolecular squaramide-based matrix can support HepG2 early proliferation and differentiation with the expression of several key metabolic enzymes and hepatic markers to a greater extent than Matrigel.

A fully synthetic and bioactive squaramide-based supramolecular hydrogel material bearing RGD peptides was prepared for 3D cell culture. The co-assembly approach of the synthesized monomers **1** and **2** to prepare the hydrogel materials enables tuning of the peptide concentration within the materials. The RGD-functionalized squaramide-based hydrogels were demonstrated to be optically clear, mechanically soft, and self-recovering. Encapsulated cells recognize the RGD peptides (0.15–0.45 mM) embedded within the network by spreading, initiating actin polymerization, and inducing cell migration in 3D. These RGD-functionalized squaramide hydrogels support the growth of HepG2 cells into compact spheroids with high cell viability, active proliferation, and differentiation, resulting in significantly higher gene expression of metabolic enzymes and hepatic markers as well as the formation of liver structures and basal-lateral polarization. This chemically well-defined monomers enable a facile preparation protocol through their co-assembly, cytocompatibility, and capacity to trigger differentiation on par with natural materials challenging Matrigel, the current gold standard for liver spheroid culture, but can be more broadly applied in other areas of tissue culture where cell-matrix interactions are necessary to facilitate various aspects of cell behavior. Moreover, their self-recovering properties enable gentle spheroid release which can be used for downstream analysis. Finally, the terminal azide on squaramide monomer **3** leaves the door open to further chemically modification and crosslinks for future biomaterials designs, for example, tuning the stiffness of supramolecular network in a straightforward manner to provide a closer in vivo mimicking microenvironment for cells.

Experimental Section

Experimental details including synthetic procedures and characterization, oscillatory rheology, UV–vis spectroscopy, cryogenic transmission electron and confocal laser scanning microscopy, RT-PCR, and immunofluorescence analysis are described in Supporting Information.

Supporting Information

Supporting Information is available from the Wiley Online Library or from the author.

Acknowledgements

T.L. and L.v.d.B. contributed equally to this work. The authors would like to thank R.I. Koning and B. Koster for the cryo-TEM. R.E.K. would like to acknowledge the European Research Council (ERC) for her ERC grant "SupraCTRL." A.J.W. and D.H. acknowledge funding from the Fraunhofer Attract "3DNanoCell" grant. T.L. and C.T. thank the China Scholarship Council for their CSC scholarships.

Conflict of Interest

The authors declare no conflict of interest.

Data Availability Statement

The data that supports the findings of this study are available in the supplementary material of this article.

Keywords

3D cell culture, HepG2 spheroids, hydrogel s, squaramide, supramolecular

Received: October 29, 2020
Revised: March 19, 2021
Published online: April 30, 2021

[1] O. A. Almazroo, M. K. Miah, R. Venkataramanan, *Clin. Liver Dis.* **2017**, *21*, 1.
[2] R. J. Andrade, G. P. Aithal, E. S. Björnsson, N. Kaplowitz, G. A. Kullak-Ublick, D. Larrey, T. H. Karlsen, *J. Hepatol.* **2019**, *70*, 1222.
[3] G. A. Kullak-Ublick, R. J. Andrade, M. Merz, P. End, A. Benesic, A. L. Gerbes, G. P. Aithal, *Gut* **2017**, *66*, 1154.
[4] J. A. Heslop, C. Rowe, J. Walsh, R. Sison-Young, R. Jenkins, L. Kamalian, R. Kia, D. Hay, R. P. Jones, H. Z. Malik, S. Fenwick, A. E. Chadwick, J. Mills, N. R. Kitteringham, C. E. P. Goldring, B. Kevin Park, *Arch. Toxicol.* **2017**, *91*, 439.
[5] C. Rowe, D. T. Gerrard, R. Jenkins, A. Berry, K. Durkin, L. Sundstrom, C. E. Goldring, B. K. Park, N. R. Kitteringham, K. P. Hanley, N. A. Hanley, *Hepatology* **2013**, *58*, 799.
[6] H. H. J. Gerets, K. Tilmant, B. Gerin, H. Chanteux, B. O. Depelchin, S. Dhalluin, F. A. Atienzar, *Cell Biol. Toxicol.* **2012**, *28*, 69.
[7] C. S. Hughes, L. M. Postovit, G. A. Lajoie, *Proteomics* **2010**, *10*, 1886.
[8] S. C. Ramaiahgari, M. W. Den Braver, B. Herpers, V. Terpstra, J. N. M. Commandeur, B. Van De Water, L. S. Price, *Arch. Toxicol.* **2014**, *88*, 1083.
[9] S. Hiemstra, S. C. Ramaiahgari, S. Wink, G. Callegaro, M. Coonen, J. Meerman, D. Jennen, K. van den Nieuwendijk, A. Dankers, J. Snoeys, H. de Bont, L. Price, B. van de Water, *Arch. Toxicol.* **2019**, *93*, 2895.
[10] K. R. Stevens, J. S. Miller, B. L. Blakely, C. S. Chen, S. N. Bhatia, *J. Biomed. Mater. Res., Part A* **2015**, *103*, 3331.
[11] M. M. Malinen, H. Palokangas, M. Yliperttula, A. Urtti, *Tissue Eng., Part A* **2012**, *18*, 2418.
[12] H. Jeon, K. Kang, S. A. Park, W. D. Kim, S. S. Paik, S. H. Lee, J. Jeong, D. Choi, *Gut Liver* **2017**, *11*, 121.
[13] N. S. Bhise, V. Manoharan, S. Massa, A. Tamayol, M. Ghaderi, M. Miscuglio, Q. Lang, Y. S. Zhang, S. R. Shin, G. Calzone, N. Annabi, T. D. Shupe, C. E. Bishop, A. Atala, M. R. Dokmeci, A. Khademhosseini, *Biofabrication* **2016**, *8*, 014101.
[14] J. Christoffersson, C. Aronsson, M. Jury, R. Selegård, D. Aili, C. F. Mandenius, *Biofabrication* **2019**, *11*, 015013.

[15] M. Krüger, L. A. Oosterhoff, M. E. van Wolferen, S. A. Schiele, A. Walther, N. Geijsen, L. De Laporte, L. J. W. van der Laan, L. M. Kock, B. Spee, *Adv. Healthcare Mater.* **2020**, *9*, 1901658.
[16] B. J. Klotz, L. A. Oosterhoff, L. Utomo, K. S. Lim, Q. Vallmajo-Martin, H. Clevers, T. B. F. Woodfield, A. J. W. P. Rosenberg, J. Malda, M. Ehrbar, B. Spee, D. Gawlitta, *Adv. Healthcare Mater.* **2019**, *8*, 1900979.
[17] S. Ye, J. W. B. Boeter, M. Mihajlovic, F. G. van Steenbeek, M. E. van Wolferen, L. A. Oosterhoff, A. Marsee, M. Caiazzo, L. J. W. van der Laan, L. C. Penning, T. Vermonden, B. Spee, K. Schneeberger, *Adv. Funct. Mater.* **2020**, *30*, 2000893.
[18] G. Sorrentino, S. Rezakhani, E. Yildiz, S. Nuciforo, M. H. Heim, M. P. Lutolf, K. Schoonjans, *Nat. Commun.* **2020**, *11*, 3416.
[19] M. Kumar, B. Toprakhisar, M. Van Haele, A. Antoranz, R. Boon, F. Chesnais, J. De Smedt, T. I. Idoype, M. Canella, P. Tilliole, J. De Boeck, T. Tricot, M. Bajaj, A. Ranga, F. M. Bosisio, T. Roskams, L. A. van Grunsven, C. M. Verfaillie, *bioRxiv: 2020.09.03.280883*, **2020**.
[20] M. J. Webber, E. A. Appel, E. W. Meijer, R. Langer, *Nat. Mater.* **2015**, *15*, 13.
[21] C. L. Maikawa, A. A. A. Smith, L. Zou, G. A. Roth, E. C. Gale, L. M. Stapleton, S. W. Baker, J. L. Mann, A. C. Yu, S. Correa, A. K. Grosskopf, C. S. Liong, C. M. Meis, D. Chan, M. Troxell, D. M. Maahs, B. A. Buckingham, M. J. Webber, E. A. Appel, *Nat. Biomed. Eng.* **2020**, *4*, 507.
[22] D. Straßburger, N. Stergiou, M. Urschbach, H. Yurugi, D. Spitzer, D. Schollmeyer, E. Schmitt, P. Besenius, *ChemBioChem* **2018**, *19*, 912.
[23] S. Spaans, P. P. K. H. Fransen, M. J. G. Schotman, R. Van Der Wulp, R. P. M. Lafleur, S. G. J. M. Kluijtmans, P. Y. W. Dankers, *Biomacromolecules* **2019**, *20*, 2360.
[24] Y. Wang, K. M. Dillon, Z. Li, E. W. Winckler, J. B. Matson, *Angew. Chem.* **2020**, *59*, 16841.
[25] J. Ramos, S. Arufe, H. Martin, D. Rooney, R. B. P. Elmes, A. Erxleben, R. Moreira, T. Velasco-Torrijos, *Soft Matter* **2020**, *16*, 7916.
[26] L. A. Marchetti, L. K. Kumawat, N. Mao, J. C. Stephens, R. B. P. Elmes, *Chemistry* **2019**, *5*, 1398.
[27] C. López, M. Ximenis, F. Orvay, C. Rotger, A. Costa, *Chem.: Eur. J.* **2017**, *23*, 7590.
[28] E. Castellanos, B. Soberats, S. Bujosa, C. Rotger, R. De Rica, A. Costa, *Biomacromolecules* **2020**, *21*, 966.
[29] V. Saez Talens, P. Englebienne, T. T. Trinh, W. E. M. Noteborn, I. K. Voets, R. E. Kieltyka, *Angew. Chem.* **2015**, *127*, 10648.
[30] V. Saez Talens, D. M. M. Makurat, T. Liu, W. Dai, C. Guibert, W. E. M. Noteborn, I. K. Voets, R. E. Kieltyka, *Polym. Chem.* **2019**, *10*, 3146.
[31] C. Tong, T. Liu, V. Saez Talens, W. E. M. Noteborn, T. H. Sharp, M. M. R. M. Hendrix, I. K. Voets, C. L. Mummery, V. V. Orlova, R. E. Kieltyka, *Biomacromolecules* **2018**, *19*, 1091.
[32] V. Saez Talens, G. Arias-Alpizar, D. M. M. Makurat, J. Davis, J. Bussmann, A. Kros, R. E. Kieltyka, *Biomacromolecules* **2020**, *21*, 1060.
[33] K. D. Park, R. Liu, H. Kohn, *Chem. Biol.* **2009**, *16*, 763.
[34] C. H. Yu, J. B. K. Law, M. Suryana, H. Y. Low, M. P. Sheetz, *Proc. Natl. Acad. Sci., U. S. A.* **2011**, *108*, 20585.
[35] P. T. Caswell, T. Zech, *Trends Cell Biol.* **2018**, *28*, 823.
[36] K. M. Hakkinen, J. S. Harunaga, A. D. Doyle, K. M. Yamada, *Tissue Eng., Part A* **2011**, *17*, 713.
[37] H. Liu, M. Wu, Y. Jia, L. Niu, G. Huang, F. Xu, *NPG Asia Mater* **2020**, *12*, 45.
[38] F. van Zijl, W. Mikulits, *World J. Hepatol.* **2010**, *2*, 1.
[39] S. E. Kim, S. Y. An, D. H. Woo, J. Han, J. H. Kim, Y. J. Jang, J. S. Son, H. Yang, Y. P. Cheon, J. H. Kim, *Stem Cells Dev.* **2013**, *22*, 1818.
[40] D. S. Reynolds, K. M. Tevis, W. A. Blessing, Y. L. Colson, M. H. Zaman, M. W. Grinstaff, *Sci. Rep.* **2017**, *7*, 10382.
[41] A. Asthana, W. S. Kisaalita, *Drug Discov. Today* **2012**, *17*, 810.
[42] X. Cui, Y. Hartanto, H. Zhang, *J. R. Soc. Interface* **2017**, *14*, 20160877.
[43] T. A. Brieva, P. V. Moghe, *Biotechnol. Bioeng.* **2004**, *85*, 283.
[44] R. Z. Lin, L. F. Chou, C. C. M. Chien, H. Y. Chang, *Cell Tissue Res.* **2006**, *324*, 411.
[45] R. Akasov, D. Zaytseva-Zotova, S. Burov, M. Leko, M. Dontenwill, M. Chiper, T. Vandamme, E. Markvicheva, *Int. J. Pharm.* **2016**, *506*, 148.
[46] Y. Miyamoto, M. Ikeuchi, H. Noguchi, T. Yagi, S. Hayashi, *Cell Med.* **2015**, *8*, 47.
[47] T. Nishikawa, Y. Tanaka, M. Nishikawa, Y. Ogino, K. Kusamori, N. Mizuno, Y. Mizukami, K. Shimizu, S. Konishi, Y. Takahashi, Y. Takakura, *Biol. Pharm. Bull.* **2017**, *40*, 334.